THE USE OF THE HILBERT-HUANG TRANSFORM IN THE AUTOMATED DETECTION OF VENOUS GAS EMBOLI

Chappell M.A., Payne S.J.
Department of Engineering Science, University of Oxford, Parks Road, Oxford, OX1 3PJ, UK

Introduction

Decompression sickness (DCS) is a risk to anyone who exposes themselves to significant changes in atmospheric pressure e.g. SCUBA divers, astronauts. It arises through the formation of gas phase in the body through the release of gas dissolved in the tissues at a higher atmospheric pressure. Some of this gas phase is liberated into the blood, so called Venous Gas Emboli (VGE). This may be detected in the pulmonary artery using ultrasound techniques. The cheapest method of VGE detection uses a simple Doppler ultrasound device operating at 2-5MHz. In these systems ultrasound is used to irradiate the pulmonary artery; the reflected radiation is shifted in frequency according to the Doppler Principle. VGE are highly reflective to the ultrasound radiation because they contain a gas-liquid interface. The reflected ultrasound signal is demodulated to remove the carrier frequency, leaving only the frequency shift component, which appears as an audio signal. Currently this signal is then classified by a trained observer, making the process time-consuming and highly subjective [9]. The automated detection, however, has been confounded by the presence of signals arising from the movement of red blood cells in response to the heart beat. The aim of this study was to investigate whether the signals arising from blood cells and VGE were separable under the Hilbert-Huang transform (HHT) [5], such that information about the number and nature of VGE could be automatically extracted from the signal.

Method

Doppler ultrasound signals from recreational SCUBA divers, post-decompression, were provided by DAN Europe. The HHT was performed using the HHT-DPS software program provided by NASA. The HHT decomposes the signal into a series of components called Intrinsic Mode Functions (IMF). Each IMF represents locally one oscillatory mode in the data, hence the full set of IMF for one signal represents a basis set for that signal. However, unlike the basis set of Fourier Transforms there is no requirement for the IMF to be sinusoidal or even stationary. To ensure that an IMF represents oscillatory modes of the data the following two conditions need to be satisfied [5]:

- The number of extrema and number of zero crossings must either be equal to or differ by at most one.
- At any point the mean value of the envelope defined by the local maxima and the envelope defined by the local minima is zero.

Ideally the second condition should be that the local mean of the IMF is zero. However, this would involve the definition of a local time scale which is impossible to define [5]. These conditions ensure that the IMF in each cycle, defined by the zero crossings, involves only a single mode of oscillation.

To generate the IMF from data the Empirical Mode Decomposition (EMD) is employed [5]. Firstly, the extrema of the data are identified, then the envelopes of maxima and minima are created using cubic spline fitting. The mean of the two envelopes is designated m_1 and the difference between the data, x, and m_1 is the first component h_1, i.e.:

$$h_1(t) = x(t) - m_1(t).$$

Ideally h_1 should be an IMF by the definition given earlier. However, in practice this will not necessarily be the case, see [4, 5] for details. Consequently the sifting process described above is repeated: in the second sifting h_1 is treated as the data so that:

$$h_{11}(t) = h_1(t) - m_{11}(t).$$

This procedure is repeated k times, until h_{1k} is an IMF:

$$h_{1k}(t) = h_{1(k-1)}(t) - m_{1k}(t),$$

which is then designated as:

$$c_1(t) = h_{1k}(t).$$

If the sifting process was continued ad-infinitum eventually the component, k_{1k}, would become a pure frequency modulated signal of constant amplitude, and the physically meaningful amplitude fluctuations would be obliterated [5]. To avoid this the sifting process is stopped once the number of zero crossings and extrema remains the same for S successive sifting steps. Since it has been found that a value of $3 < S < 5$ typically yields a successful result [4], S=3, the default value in the HHT-DPS, is adopted for this study.

c_1 should then contain the finest scale, i.e. the shortest period, in the data and is separated from the signal:

$$r_1(t) = x(t) - c_1(t),$$

to give a residue, r_1, which contains information about longer period components. It is thus treated as new data and subjected to the same sifting process described above. This procedure is repeated until a predetermined criteria is met: either no more IMF can be extracted because the remaining residue is monotonic, or the residue is so small that it is insignificant.

The final result is thus:

$$x(t) = \sum_{i=1}^{n} c_i(t) + r_n(t),$$

where the signal has been decomposed into n-empirical modes and a residue, which is either a mean trend or constant.

The HHT is particularly suitable for analysing non-stationary signals because the basis functions for the HHT are based on the signal itself [5]; each IMF thus captures a different scale in the original signal. It is found when the Doppler audio data is processed using the HHT that IMF corresponding to smaller scales contain patterns from both the VGE and blood cell movement. However, IMF of a larger scale are dominated by the presence of VGE only.

A typical Doppler signal of length 70 s is found to produce of the order of 20 IMF. Since, of these, the VGE patterns are most significant, as compared with blood cell movement, in the 6^{th} – 10^{th} IMF, the 6^{th} IMF is chosen for further analysis. In practice it is possible to halt the process once the required number of IMF have been extracted, it being computationally advantageous to extract no more than the necessary components.

The relevant IMF are subsequently processed to detect the VGE. A method of peak detection is applied, based on the technique of Hamilton and Tompkins [3], originally applied to the detection of QRS complexes in single channel ECG data. This consists of a pre-processing stage, Figure 1, as part of which peaks are detected that exceed a threshold based on a fraction of the median of the previous five detected peaks. Different fractions are used to detect the start and end of the section, based on a modification of the original technique [1]. When detecting the start of a peak a fractional value of 0.6 is used, the end being detected using a fractional value of 0.3, with the location of the peak marked as the maximum point in this interval. This method ensures that only distinct peaks, separate in time, are detected, making the technique robust toward local maxima.

Since the time duration of a VGE passing the Doppler probe is of the order of 10 ms, the use of a 12.5 ms time average should allow this method to separate individual VGE, in the original signal.

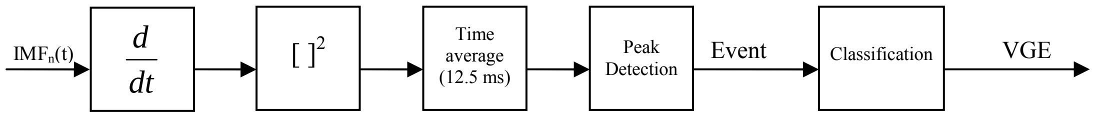

Figure 1: Processing an IMF to identify VGE

Peaks detected by this method are events in the IMF. However, these events are not solely appearances of VGE: for example the HHT process does not necessarily remove all contributions from blood cell movement even in larger scale IMF; consequently some peaks detected may correspond to peak blood movements, which occur during the systole phase of the heart cycle. Further processing is therefore required to classify the events determined from the IMF.

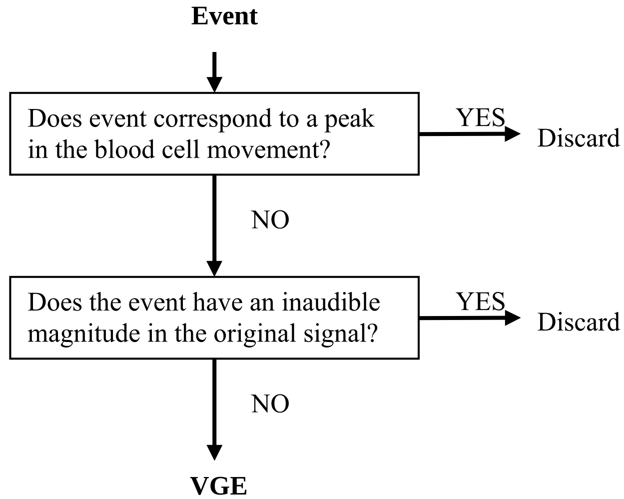

Figure 2 Flow chart for classification of an event to detect VGE

Firstly, the position of the peaks of blood movement are identified. This is achieved using the original signal, which is processed using the same peak detection method described above. This produces a list of events in the original signal, which will include the blood movement and VGE. From this list, systole events are extracted. These can be identified because they occur with a near periodic time interval. The list of systole events is compared to the events identified in the IMF and corresponding ones discarded: the first step in Figure 2.

A further type of anomalous event can be identified in the IMF. These arise through variations in the pattern of blood cell movement, and are especially prominent in signals with few VGE. These events do not correspond to VGE, because their magnitude in the original signal is below the threshold at which it could be identified as such aurally. Thus events where the magnitude in the original signal falls below the local mean of the signal magnitude, and is therefore inaudible, are discarded: the second step in Figure 2.

Results

Two recordings will be considered, both of which arise from subjects who were monitored post-decompression for a period of approximately 30 s after undertaking recreational diving. The first recording, A, shows signs in the Doppler audio of a number of VGE being present in the pulmonary circulation. In the second recording, B, there is a complete absence of sounds associated with the presence of VGE.

Figure 3a (left) shows the processed form of the 6th IMF for recording A for a short section of the recording, with peaks corresponding to VGE marked. Figure 3b (left) shows the corresponding spectrogram of the original signal; the periodic pattern associated with blood cell motion can be clearly identified, especially in the lower frequency range, whereas VGE are typically marked by high magnitudes and a larger frequency range concentrated in short time scales, of approximately 10 ms. Of particular note is the peak appearing in the processed form of the IMF, Figure 3a left, at 2.5 s, which, although having significant magnitude in the IMF, has not been identified as a VGE. This can be seen to be a correct classification by inspection of the spectrogram, Figure 3b (left), which shows no indication of a VGE. The presence of this peak in the IMF is best explained by the non-standard shape of the blood movement pattern in the spectrogram between approximately 2.5 – 3.5s. In total 27 VGE are detected by the algorithm for recording A. In general the algorithm is capable of identifying individual VGE, even when they occur successively in time. However, there is no reason why VGE must occur singly and so may their patterns may overlap in the original signal: under these circumstances the time averaging process may limit the individual identification of VGE. Such a case occurs at approximately 9 s where the spectrogram suggests that there may be three VGE, but only two are identified.

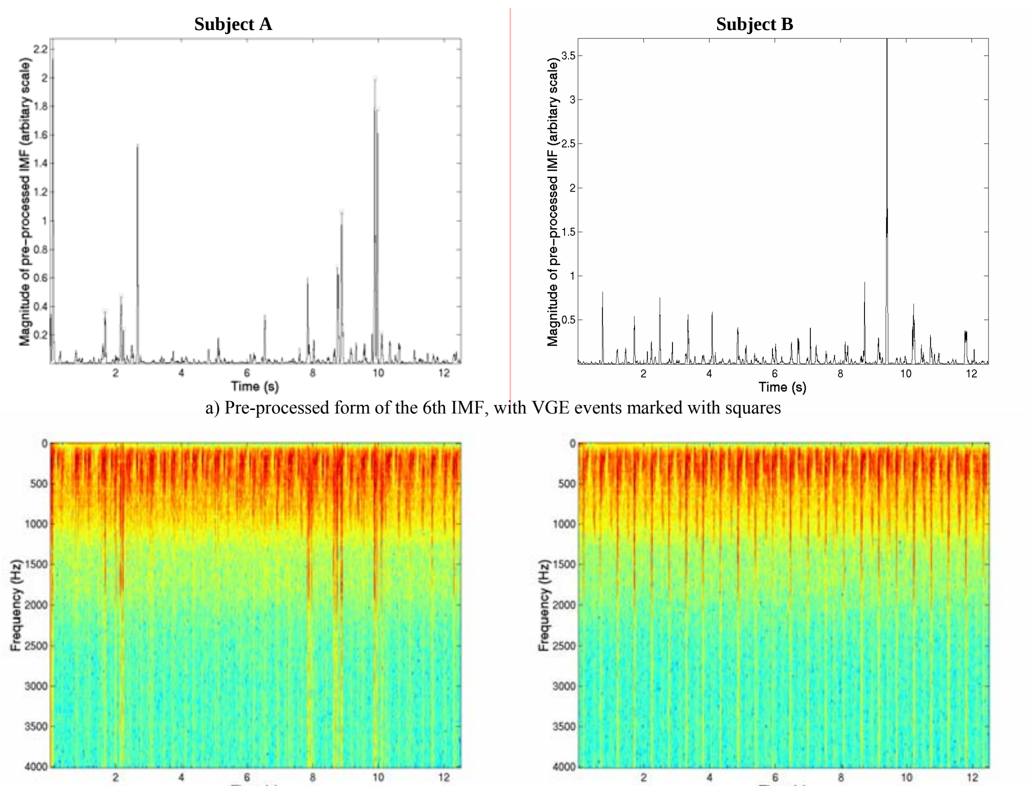

a) Pre-processed form of the 6th IMF, with VGE events marked with squares

b) The spectrogram of the original signal. Blood movement can be identified as the periodic pattern predominantly in the lower frequencies. VGE are marked by higher frequency content, with only short time duration.

Figure 3 Results of VGE detection for the first 12 s of the Doppler audio signal from subjects A and B

Figure 3a (right) shows the processed form of the 6th IMF for recording B. It can be seen that peaks appear in the processed IMF, but these events are identified by the algorithm as not being VGE, due to their characteristics. This identification can be confirmed from the spectrogram

Figure 3b (right), which only shows evidence of blood cell motion time-frequency patterns. In recording B only 1 possible VGE is identified by the algorithm.

Discussion

Doppler ultrasound signals are usually classified by an expert according to either the Spencer or Kisman-Masurel (KM) scales. The simpler of the two in definition, although not necessarily simpler to use [7]), is the Spencer Scale, Table 1. The algorithm outlined in Method produces bubble counts per unit time, but can be converted, using the estimated locations for the heart beats derived from the signal, into a standard grade. A potential implementation of this conversion has been created. The percentage of cardiac periods containing bubbles is calculated and classification made on this score. The third column of Table 1 outlines the limits used in this implementation, which have been derived empirically from the definitions. In the present implementation Grade IV is ignored because it is not easily assessed on percentage of cardiac periods containing bubbles alone, and the available data does not contain any of these grades for verification. Additionally, a small number of VGE are permitted in Grade 0; this is something of a compromise, because it is not always possible to remove all anomalous non-VGE events by the method outlined above.

TABLE 1: THE SPENCER SCALE (FROM [8]), THE THIRD COLUMN SHOWING EMPIRICALLY DERIVED LIMITS USED HERE FOR AUTOMATIC GRADING

Grade	Spencer code	Proportion of cardiac periods containing VGE, p (%)
0	A complete lack of bubble signals.	$p < 2$
I	An occasional bubble signal discernable with the cardiac motion signal with the great majority of cardiac periods free of bubbles.	$2 < p < 10$
II	Many, but less than half, of the cardiac periods contain bubbles, singly or in groups.	$10 < p < 50$
III	Most of the periods contain showers of single-bubble signals, but not dominating or over-riding the cardiac motion signals.	$50 < p$
IV	The maximum detectable bubble signal sounding continuously throughout systole and diastole of every cardiac period, and over-riding the amplitude of normal cardiac signals.	-

The alternative grading scheme, KM scale, was originally designed for computer implementation [8]. Therefore, an automatic grading scheme based on this code should be feasible. A preliminary system, based on the KM scheme for resting subjects, has thus been implemented. The KM grade is based on three parameters:

- Frequency (f): The number of VGE per cardiac period, Table 2. In the automatic implementation the number of VGE in each cardiac period is determined, resulting in a 'code' for each period. The most commonly occurring code, excluding '0', is chosen to be representative. Note that code 4 is not realisable under this scheme, for similar reasons that limited the implementation of grade IV on the Spencer scale: that this code is not easily defined from the percentage of cardiac periods containing VGE, and no data of this type was available for verification.
- Percentage (p): The number of cardiac periods containing VGE (resting subject), Table 2. This can be implemented directly using the calculated percentage of cardiac periods containing VGE and the limits provided.
- Amplitude (A): A comparison of the audible amplitude of VGE to heart cycle sounds, Table 3. This is implemented by a comparison of the mean magnitude of VGE in the signal to the mean magnitude of identified peaks of bubble movement. The limits used in the automatic grading routine for this parameter are shown in the right-hand column of Table 3, these have been derived empirically and represent the authors' best estimate at this stage.

The code produced is then converted to a grade using a standard table [8]. Like the Spencer scale these grades range from 0 to IV, but incorporate '+' and '-' modifiers to give a greater gradation. In practice some codes are impossible or unlikely to occur, with only about 64 of the possible combinations being useable for the precordial site [8].

TABLE 2: KM FREQUENCY PARAMETER AND PERCENTAGE PARAMETER [8]

Code	Frequency (f) – bubbles per cardiac period	Rest percentage cardiac periods, p (%)
0	0	0
1	1 – 2	1 – 10
2	Several, 3 – 8	10 – 50
3	Rolling drumbeat, ≥ 9	50 – 99
4	Continuous sound	100

TABLE 3: KM AMPLITUDE PARAMETER [8], THE THIRD COLUMN SHOWING EMPIRICALLY DERIVED LIMITS USED FOR AUTOMATIC GRADING

Code	Amplitude (A)	Ratio of mean VGE amplitude to mean peak blood movement magnitude
0	No bubbles discernable	$A = 0$
1	Barely perceptible, $A(b) << A(c)$	$0 < A < 0.3$
2	Moderate amplitude, $A(b) < A(c)$	$0.3 < A < 0.9$
3	Loud, $A(b) \approx A(c)$	$0.9 < A < 3$
4	Maximal, $A(b) > A(c)$	$3 < A$

Both of these systems have been tested on a sample of 34 Doppler audio recordings from 2 subjects. These have been provided by DAN Europe and are taken from recreation divers post-decompression, representing a small fraction of the database collected under Project Safe Dive [6]. The nature of the activity from which these signals arises means that these signals are expected to exhibit only low VGE grades. All of the 34 signals could be graded by the algorithm and the results are given in Figure 4. On only one occasion was a KM code found that is classed as rarely observed. The Spencer code derived from the data was compared with that derived indirectly from the KM grade, using the conversion given in [8]. In two cases the KM code could not be converted because the code is not explicitly given, otherwise complete agreement was found. This indicates that the two schemes are being applied consistently as the Spencer scale is a subset of the KM scale [7]. It was found that the number of Spencer grade I compared to grade II could be varied with only small alterations of the boundary between them, suggesting that his will be the most critical future verification. Without the appropriate expert gradings these results represent a proof-of concept; that this system can produce reasonable and unique gradings under the standard methods from Doppler audio data. Future work will see a larger database with attached labels being used to refine and to verify the implementation set out here.

A further important consideration for VGE detection is determination of VGE size. In principle for bubbles above resonant size, of the order of 1μm at 2-5MHz [2], the relationship between reflected ultrasound intensity and bubble size should be linear [8]. It is, therefore, theoretically possible to size detected bubbles from the magnitude of the associated signal, although practical limitations such as the attenuation of the ultrasound signal through the body may make accurate size determination difficult [8]. It is yet to be determined whether size information can be extracted from the magnitude of the IMF alone, which, because the blood cell movement signal is substantially removed from the appropriate IMF, would potentially lead to a more accurate determination. Further calibration and experimentation will be required to verify and to calibrate the VGE sizing procedure.

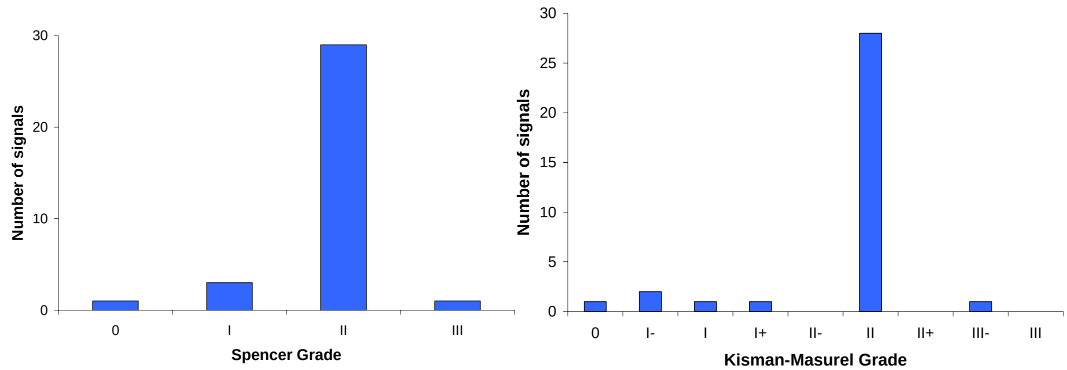

Figure 4 Spencer (left) and Kisman-Masurel (right) gradings for 34 Doppler audio signals from recreational divers post-decompression, using an automatic grading system.

Conclusion

The HHT offers a method by which Doppler ultrasound data may be analysed and the patterns due to VGE identified independently of the patterns due to blood cell movement. This will offer the possibility of an automatic grading system, in place of the current manual technique. In the future this technique also offers the promise of more accurate information about VGE including actual occurrence rate and size.

Acknowledgements

The authors would like to thank DAN Europe and the Diving Safety Laboratory for the provision of Doppler ultrasound signals.

This work was accomplished through the authorized use of the National Aeronautics and Space Administration's Hilbert-Huang Transform (HHT) (GSC-14591-1). The authors wish to acknowledge and thank NASA and the inventor, Dr. Norden Huang, for their work in this area and assistance. See http://techtransfer.gsfc.nasa.gov/HHT/hht.htm for more information on NASA's HHT.

References

1. Clifford GD, Signal Processing Methods for Heart Rate Variability [DPhil]. Department of Engineering Science, University of Oxford: Oxford; 2002.

2. Eatock BC, Nishi RY, Johnston GW, Numerical Studies of the Spectrum of Low-Intensity Ultrasound Scattered by Bubbles. Journal of the Acoustical Society of America 1985; 77 (5):1692-701.

3. Hamilton P, Tompkins W, Quantitative Investigation of QRS Detection Rules Using the MIT/BIH Arrythmia Database. IEEE Transactions on Biomedical Engineering 1986; BME-33 (12).

4. Huang NE, Man-Li CW, Long SR, Shen SP, Wendong Q, Gloersen P, Fan KL, A Confidence Limit for the Empirical Mode Decomposition and Hilbert Spectral Analysis. Proceedings of the Royal Society of London: Series A 2003; 459:2317-45.

5. Huang NE, Shen Z, Long SR, Wu MC, Shih HH, Zheng Q, Yen N, Tung CC, Liu HH, The Empirical Mode Decomposition and the Hilbert Spectrum for Nonlinear Time Series Analysis. Proceedings of the Royal Society of London: Series A 1998; 454:903-95.

6. Marroni A, Cali Corleo R, Denoble P, Understanding the Safety of Recreational Diving. DAN Europe's Project SAFE DIVE Phase I: Fine Tuning of the Field Research Engine and Methods. In International Joint Meeting on Hyperbaric and Underwater Medicine, 4-8 September. Milano; 1996. p. 279-84.

7. Nishi RY, Doppler Evaluation of Decompression Tables. In: Y-C Lin; KK Shida, editors. Man in the Sea. Vol. 1: Best Publishing Company; 1990; p. 297-316.
8. Nishi RY, Brubakk AO, Eftedal OS, Bubble Dectection. In: AO Brubakk; TS Neuman, editors. Bennett and Elliott's Physiology and Medicine of Diving. 5th edn: Saunders; 2003; p. 501-29.
9. Sawatzky KD, Nishi RY, Assessment of Inter-Rater Agreement on the Grading of Intravascular Bubble Signals. Undersea Biomedical research 1991; 18 (5-6):373-96.